ASTFE American Society of Thermal and Fluids Engineers

5th Thermal and Fluids Engineering Conference (TFEC)
April 5–8, 2020 New Orleans, LA , USA

TFEC-2020-32269

STUDY OF THERMAL AND MASS TRANSFER CHARACTERISTICS ON AIR GAP DIFFUSED DESALINATION

WANG Ping, YU Bingchen, CHEN Lele, XU Shiming*, XU Lin, ZHANG Shuping, LI Lei

Key Laboratory of Ocean Energy Utilization and Energy Conservation of Ministry of Education, School of Energy and Power Engineering, Dalian University of Technology, Dalian 116024, China

ABSTRACT

In this paper, the diffusion-gap seawater desalination is modeled and analyzed. A mathematical model is established by the conservation of mass and energy. The CFD software is adopted to realize the two-dimensional simulation of water vapor in the air gap. The water evaporate on the evaporator and the vapor diffusion through the air gap, condense on the condenser. The appropriate simplification and user-defined functions were used to assist the study. A steady-state numerical simulation of the water vapor diffusion process in the air gap is carried out and the model height is 0.5 m, air gap width is 5 mm and the flow rate is 0.005 kg/s; by the distribution of temperature, pressure, water vapor concentration in the air gap, it is conducive to know the microscopic flow within the air gap.

KEY WORDS: Air gap, Diffusion, Thermal and mass transfer

1. INTRODUCTION

Many scholars have used CFD methods to study the topic of falling film evaporation or condensation or membrane distillation. Leu et al. [1] simulated the heat and mass transfer of liquid film evaporation on a vertical plate covered with porous media. They believe that the amount of latent heat transfer in heat transfer is more than sensible heat transfer, and the smaller porosity and thinner thickness can promote interface temperatures and mass concentrations higher, thus enhancing heat and mass transfer through the liquid film. Ming-Hsyan et al. [2] studied the effect of Darcian resistance on mixed convection when fluid evaporation on porous media. They show that when the Darcian resistance is small, the buoyancy increases gradually, the overall heat transfer rate is cut off, and the fluid evaporation on the wall increases. Yiotis et al. [3] studied the effect of film flow on the drying of porous media. The results show that the film flow is the main influencing factor of the drying of porous materials. When the capillary action controls the whole process, the influence of film flow plays a leading role. In contrast, viscous flow plays a minor role. The results of the study were applied to the drying under temperature gradient. Shirazian et al. [4] established a 3d model to simulate the transmission of water vapor through the membrane, and used finite element method to solve the governing equation, the distribution of concentration and temperature is obtained. The simulation results are consistent with the experimental results. At the same time, the author simulated the evaporation performance under different operating parameters and membrane properties. The results show that the gas flow rate is beneficial

*Corresponding author. E-mail address: xsming@dlut.edu.cn

to break the thermodynamic equilibrium and is an important parameter affecting the evaporation rate. Tang et al. [5] studied the gas-liquid multiphase flow problem in vacuum membrane distillation, using the computational fluid software Fluent to simulate the transfer of heat and mass through the porous membrane. In the simulation, the aqueous solution of sodium chloride is considered to be a continuous, incompressible fluid. During the phase transfer process, each part is in a state of local thermal equilibrium, and the volumetric flow rate of water vapor at different feed temperatures is calculated in the simulation simultaneously. Wang et al. [6] proposed a flat-plate splitter, a pyramidal splitter and a dome-shaped splitter in order to make the feed in the cross-flow vacuum membrane distillation uniform and improve the performance, the performance of the three types of splitter were compute The results show that the pyramidal splitter and the dome-shaped splitter are better than the flat-plate splitter. Ma Le [7] designed a new type of solar desalination device based on the seawater desalination device. According to theoretical analysis, the solar seawater desalination efficiency is improved by improving the traditional solar desalination device. The numerical simulation method is adopted to simulate the seawater desalination process. The distribution of temperature field, velocity field and pressure field inside the device have an important guiding role in the study. Liu Jun [8, 9] used Fluent to study the process of the hollow fiber decompression membrane distillation. The model simulation results were consistent with the experimental results. The author analyzed the influence of operating conditions on the distribution of heat and mass parameters, such as the feed rate, temperature and vacuum degree, and the effects of porous membrane properties on membrane flux including porosity and tortuosity. Xu Kai [10] used Fluent software to simulate the internal heat and mass transfer process of a new heat recovery plate frame air gap membrane distillation module, and investigated the internal temperature distribution of the flow field under different feed temperatures, flow rates and vacuum levels. The intuitive parameter distribution rules inside the components, which lay the foundation for further optimization of the internal structure.

2. MODEL OF WATER VAPOR DIFFUSION

In this paper, the two-dimensional simulation of the diffusion flow field of wet air in the air gap is carried out. Simulation of the thermal diffusion process of water vapor in the air gap is achieved in the fluent software by using species transport model and importing user-defined functions.

2.1 Physical Models and Boundary Conditions

As shown in Fig. 1, the air gap diffusion seawater desalination device is mainly composed of two flat plates which are close and in parallel with each other. One of the flat plates is filled with porous medium, which act as evaporator, and the another plate has a flow channel where the cold water flows, which act as condenser. When the device operate, cold water flows from the bottom of the condenser, flows upward along the flow channel, flows out at the top of the condenser, and then heated by the external heat source, and the hot water flows into the porous medium in evaporation, flowing through the evaporator from top to bottom under the action of gravity. Due to the heating of the external heat source, the temperature of the water in the evaporator is higher than the water in the condenser, and the partial pressure of saturated water vapor in the surface of the evaporator is greater than the surface of the condenser, the partial pressure of water vapor on the evaporator is greater than the condenser. Water vapor evaporates from the evaporator under the driven of pressure differential and diffuses through the air gap to condense on the condenser. When the water evaporates on the evaporator, the latent heat is taken away, and the temperature of the fluid is lowered. On the condenser, latent heat is released to heat the cold fluid in the condenser to realize energy recovery and utilization. Since the latent heat of vaporization and condensation is approximately the same, the temperature

difference between the fluid in the evaporator and the condenser at the same height is substantially constant, and the existence of this temperature difference makes the evaporation and condensation process of water proceed in the entire height direction. The device operates under atmospheric pressure and is insulated from the external environment by wrapping the insulation layer outside the device, when the process is in steady state operation, the evaporator boundary and the condenser boundary temperature are coupled to each other. Compared with the air gap membrane distillation seawater desalination (AGMD), the gap-diffusion seawater desalination cancel the presence of a membrane, and retain the advantages of membrane distillation, seawater evaporates on the surface of the porous medium and then enters the air gap. The parameters at inlet of evaporator and condenser are known.

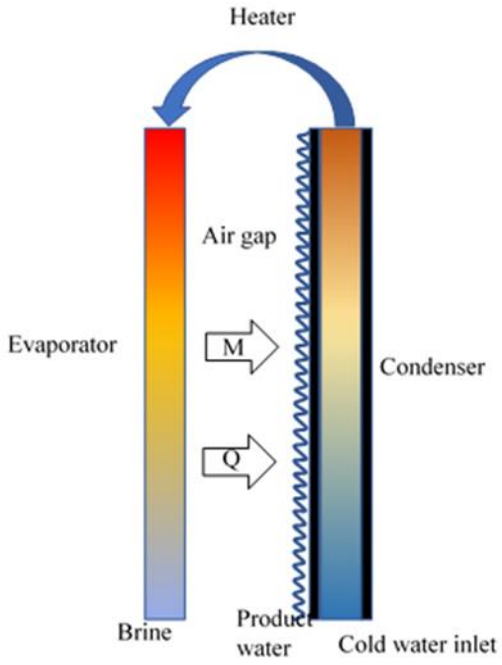

Fig. 1 The flow diagram of air gap diffusion desalination unit (M: mass transfer, Q: heat transfer)

Boundary conditions and governing equations are two necessary conditions to analyze hydrodynamic problems. When the boundary conditions of fluids are determined, the distribution of the flow field can be obtained. Figure 2 shows the diffusion of water vapor in the air gap and the coordinate setting. The model height is 0.5m and the air gap width is 5mm. the boundary conditions of the upper and lower ports of the air gap are adiabatic wall, the boundary conditions of the surface of the evaporator and the condenser are fixed temperature, and the wall temperature is calculated by numerical simulation. The interface temperature calculated by the simulation fitted with quartic function, and the fitting formula is as follows. The comparison between the fitting result and the calculation result is shown in Fig. 3.

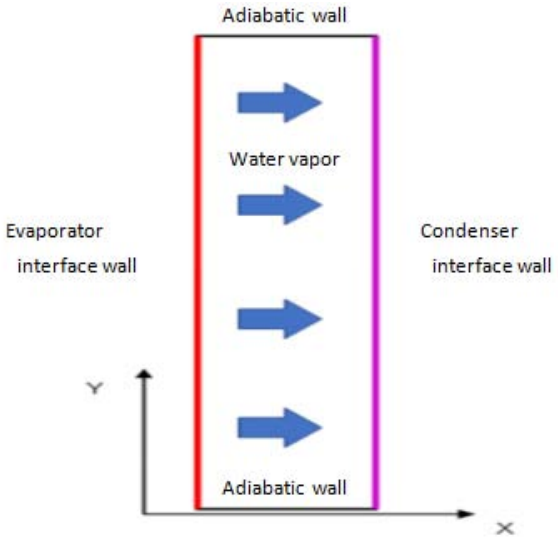

Fig. 2 Boundary conditions

$$T = ay^4 + by^3 + cy^2 + dy + e \tag{1}$$

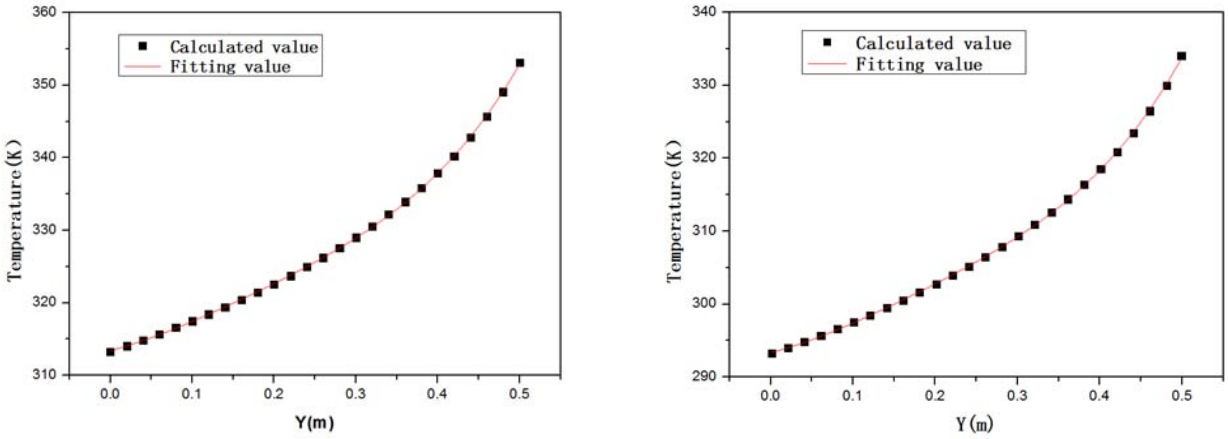

(a)Evaporator (b) Condenser

Fig. 3 Temperature on the interface

2.2 The Mathematical Model

Computational fluid dynamics studies complex hydrodynamic problems by discretizing fluids, solving mass conservation equations, momentum equations, energy equations, and transport equations for each micro-element. The expressions for each equation are as follows. In this paper, we imported UDF, and add mass source S_m, momentum source S_v, energy source S_h and component source S_i to the DEFINE_SOURCE to simulate the evaporation and condensation process of water vapor.

Mathematical model is based on the following assumptions:

(1) Water vapor is the ideal gas;

(2) The model is in the steady state condition;

(3) Air gap pressure is atmospheric pressure;

(4) Ignoring the effect of porous media on the diffusion and evaporation process;

(5) No change in physical properties perpendicular to the paper surface.

2.2.1 The Govern Equation

(1) The continuity equation

$$\nabla \cdot (\rho \vec{v}) = S_m \tag{2}$$

Where S_m is the mass source.

(2) The momentum equation

$$\nabla \cdot (\rho \vec{v}\vec{v}) = -\nabla p + \nabla (\bar{\bar{\tau}}) + \rho \vec{g} + S_v \tag{3}$$

Where p is static pressure, $\bar{\bar{\tau}}$ is the stress tensor, $\rho \vec{g}$ is the gravity volume force, S_v is the additional volume force.

(3) The energy equation

$$\nabla \cdot (\vec{v}(\rho E + p)) = \nabla \cdot (k_{eff} \nabla T - \sum_i h_i \vec{J}_i + (\bar{\bar{\tau}} \cdot \vec{v})) + S_h \tag{4}$$

The first term on the right side of the equation represents the amount of energy transfer due to heat conduction, species transfer, and turbulent dissipation; $k_{eff} = k + k_t$, k_{eff} is the effective thermal conductivity, S_h is the source of energy. On the left side of the equation, E can be calculated by the following formula:

$$E = h - \frac{p}{\rho} + \frac{v^2}{2} \tag{5}$$

As for ideal gas:

$$h = \sum_i \omega_i h_i \tag{6}$$

As for incompressible fluids:

$$h = \sum_i \omega_i h_i + \frac{p}{\rho} \tag{7}$$

$$h_i = \int_{T_{ref}}^{T} c_{p,i} dT \tag{8}$$

In the formula, the subscript i indicates the species i.

(4) The species equation [11]

$$\frac{\partial}{\partial t}(\rho \omega_i) + \nabla (\rho \vec{v} w_i) = \frac{\partial \vec{j}_i}{x_i} + R_i + S_i \tag{9}$$

In the above formula, the first term on the left side indicates the rate of mass increase of the species i in the unit volume, and the second term indicates the rate of mass increase of the species i caused by convection in the unit volume; the first term on the right side indicates the rate of mass increase of species i caused by medium diffusion in the unit volume, the second term indicates the rate of increase of mass of species i caused by chemical reaction in unit volume, and the third term is the source of species.

Where $\vec{j}_i$ is the mass flux of species i caused by the concentration gradient and temperature gradient, when the flow is in laminar flow:

$$\vec{j}_i = -\rho D_{i,m} \nabla \omega_i - \frac{D_{T,i}}{T} \cdot \nabla T \tag{10}$$

When the flow is in turbulence:

$$\vec{j}_i = -(\rho D_{i,m} + \frac{\mu}{Sc_t})\nabla \omega_i - \frac{D_{T,i}}{T}\nabla T \tag{11}$$

Where $D_{i,m}$ is the mass diffusion coefficient of species i, $D_{T,i}$ is the thermal diffusivity, and the thermal diffusivity of water vapor is solved by fluent according to the kinetic theory.

$$Sc_t = \frac{\mu}{\rho D_t} \tag{12}$$

Where Sc_t is the Schmidt number.

(5) The transport equations

$$\nabla \cdot (\rho \vec{v} Y_i) = -\nabla \cdot \vec{J}_i + S_i \tag{13}$$

Where ρ is the density, and $\vec{v}$ is velocity vector of fluid.

2.2.2 The Species Transport Model

The transfer of a substance relative to another substance is called diffusion. Diffusion includes concentration diffusion caused by concentration gradient, thermal diffusion caused by temperature gradient, pressure diffusion generated by pressure gradient, forced diffusion caused by external force .A.Fick proposed the first diffusion law of Fick using an analogy with the heat conduction equation, which is applicable to any binary solid, liquid or gas solution, and provided that the mass velocity of the mixed gas is small to negligible.The vector form of the equation as follows:

As for species i:

$$j_i = -\rho D_{ij} \nabla \omega_i \tag{14}$$

As for species j:

$$j_j = -\rho D_{ij} \nabla \omega_j \tag{15}$$

Where j_i and j_j are the mass fluxes of i and j in a particular direction, respectively, ω_i and ω_j are the mass fractions of species i and species j, respectively; D_{ij} is the diffusion coefficient of component i relative to component j, D_{ji} is the diffusion coefficient of component j relative to component i, and it is easy to prove $D_{ij}=D_{ji}$.The binary diffusion coefficient D_{ij} is related to pressure, temperature and composition. For a binary gas mixture at low pressure, D_{ij} is inversely proportional to the pressure and increases with the temperature increasing.The value of D_{ij} in this study is $D_{ij}=0.187\times10^{-9}\times T^{2.072}$, and T is the temperature.

The problem is appropriately simplified in the study of evaporation and condensation of water vapor. First, ignore the influence of the falling film on the humid air, and mainly observe the distribution of water vapor in the air gap under steady-state conditions. In the simulation, the boundary is considered as a wall condition, and the liquid film have no effect on the simulation results. Second, it is believed that evaporation and condensation only occur in the first mesh of the wall boundary. The mass source and energy source of evaporation are defined in UDF.

The power of evaporation and diffusion of water vapor in the air gap diffusion seawater desalination device is the different of the partial pressure at the interface of the evaporator and the condenser. The partial pressure of water vapor is actually the expression of the concentration of water vapor in the humid air. The method for judging the generation of water vapor is whether the concentration of water vapor in the humid air is saturated. If it is not saturated, water vapor is generated. Otherwise, no water vapor is generated.

Solving the saturated vapor pressure at wall temperature using the Antoine equation. And calculate the mass fraction of saturated water vapor using the following formula:

$$\omega = \frac{p_s}{TR\rho} \tag{16}$$

Where p_s is the saturated vapor pressure at wall temperature.

The rate of water vapor generation per unit area per unit time can be obtained by the law of Fick's law of diffusion.Adding the mass flux obtained by Fick's first law of diffusion to the convective mass flux , we can get the total mass flux,It is the mass flux passing through per unit area in a unit of time. The formula is as follows:

$$m_i = j_i + \rho_i v = \omega_i (n_i + n_j) - \rho D_{ij} \nabla \omega_i \tag{17}$$

When the phase transfer occurs, the non-condensable gas (air) does not change. Therefore, it is considered that the non-condensable gas (j in the formula) is stationary. So $n_j \approx 0$, and we can transform the above formula to get the following formula：

$$m_i = -\frac{\rho D_{ij}}{1-\omega_i} \cdot \nabla \omega_i \tag{18}$$

The mass source caused by gasification on evaporator is:

$$S_m = m_i \frac{A_{eff}}{V_{cel}} \tag{19}$$

Where ω is the mass fraction of the water vapor, A_{eff} is the effective area in the grid to phase transfer, ρ is the density of the water vapor , V_{cell} is the volume of cell, D is the diffusion coefficient of water vapor in air, and the unit is m^2/s, calculated using empirical formulas, adding the DEFINE_DIFFUSIVITY to the UDF, Transferring when defining the physical properties of the mixed fluid. The evaporation rate is added to Fluent as mass source.

The evaporation process absorbs the latent heat of evaporation, and the heat source is also added to the first mesh of the wall in the UDF. The evaporation heat source is negative due to evaporation is endothermic.

$$S_{eh} = -S_{em} \cdot r \tag{20}$$

Where r is the latent heat of water in evaporator (J/kg), S_{em} is the mass source on the evaporator interface. The condensation process is opposite to the evaporation process. When the water vapor concentration on the surface of the condenser is greater than the saturated water vapor concentration at the corresponding temperature, condensation occurs, and the condensation rate is also added to the source term using Fick's law. The condensation of water vapor, the quality source and the components source of water vapor of the condensation boundary is negative. When water vapor condenses, it releases heat, and the heat source is positive.

$$S_{cm} = S_{c\bar{i}} - \frac{\rho D}{1-\omega_W} \frac{\partial \omega}{\partial n} \Big| \Big/_W V \tag{21}$$

$$S_{ch} = -S_{cm} \cdot i \tag{22}$$

Where S_{cm} is the mass source on the surface of condenser.

The momentum source in the governing equation is calculated by equation (23).

$$S_v = S_m \vec{v} \tag{23}$$

3. CALCULATION RESULTS AND ANALYSIS

3.1 Temperature Distribution

The temperature distribution is shown in Fig. 4, in the air gap the aspect ratio of the model is large. In order to reflect the internal field distribution better, the length of width direction is magnified. Since the evaporator temperature is higher than the condenser temperature, the temperature distribution in the air gap is shown that the temperature in left higher than the right, and the isotherm is inclined to the upper right. The evaporation and condensation are strong near the upper area, and the temperature changes greatly. Therefore, the isotherms are dense and the temperature changes rapidly. As the height decreases, the isotherms become sparse and the temperature changes slowly. The isotherm near the upper part of the condensation side is the densest, and is the place where the most intense temperature change.

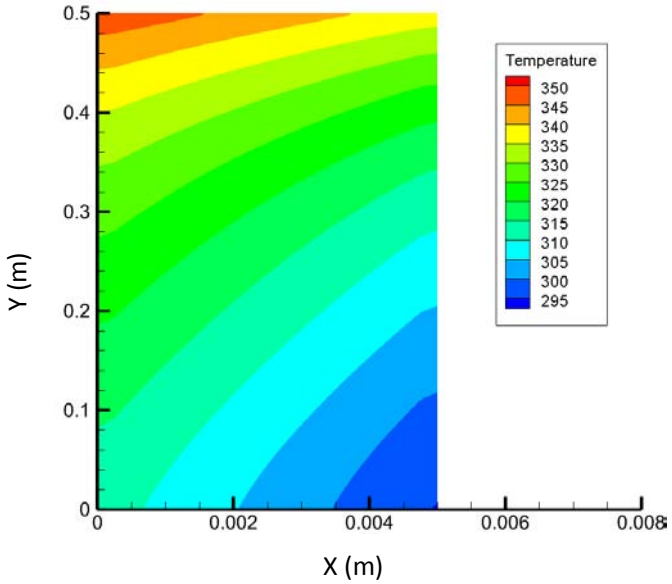

Fig. 4 Temperature distribution cloud map in air gap

As shown in Fig. 5, the temperature distribution curve at the y-coordinates of 0.125, 0.25, and 0.375 positions can be seen from the figure, in the x-direction, the temperature from the evaporator to the condenser is gradually lowered. Comparing the temperature drop in the height direction, the temperature drop in the upper half is greater than the lower halves in the same length. This shows that water evaporation is stronger in the upper part than in the lower part and the upper part is the most important area to produce fresh water. In the upper half, the fluid temperature is higher, the fluid mass transfer coefficient is larger, and the water evaporates stronger, so the temperature changes rapidly. Since the temperature difference on both sides of the air gap is basically the same, the upper, middle and lower temperature curves are parallel to each other. At the wall of the evaporator, the temperature will drop suddenly due to the evaporation is endothermic,

and the temperature of the wet air is significantly lower than the wall temperature. At the condensing wall surface, heat is accumulated at the condensation wall due to condensation of water vapor, causing the temperature of the humid air at the wall surface of the condenser higher than the wall surface of the condenser. In the air gap, the temperature is linearly distributed substantially.

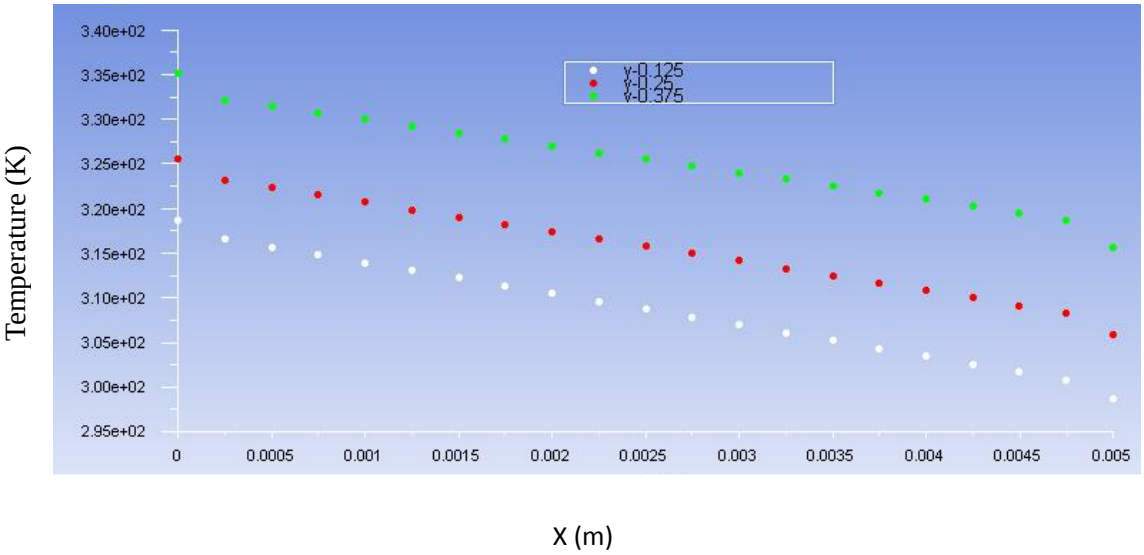

Fig. 5 Temperature distribution on different x sections

In the above mention, the temperature spurt or sudden drop due to the existence of the heat transfer and mass transfer boundary layer has negative impact on heat transfer and mass transfer in the air gap actually, and we can describe it by temperature difference polarization. Due to the existence of the boundary layer, the driving force of mass transfer in the air gap is smaller than the theoretical driving force generated by the temperature difference between the hot and cold fluids. The ratio of the temperature difference causing the driving force and the temperature difference between the hot and cold fluids is called the temperature difference polarization factor. The closer the value of the temperature difference polarization factor is to 1, the better the heat and mass transfer.

$$\theta = \frac{T_h - T_c}{T_h^0 - T_c^0} \tag{24}$$

Tab. 1 Temperature difference polarization factor on different sections

Y(m)	0.125	0.25	0.375
θ	0.7871	0.7497	0.6867

According to the working conditions studied in Fig. 5, we calculated the temperature difference polarization factors at different height positions, the results are shown in Tab 1. It can be seen from the calculation results that the temperature difference polarization factor is small at the upper position and the large at the lower position. The temperature difference polarization phenomenon is related to the strong degree of mass transfer. The more intense the evaporation and condensation, the more obvious the temperature difference polarization phenomenon, and the greater the impact on heat and mass transfer.

3.2 Pressure Distribution

Fig.6 shows the pressure distribution in the air gap.

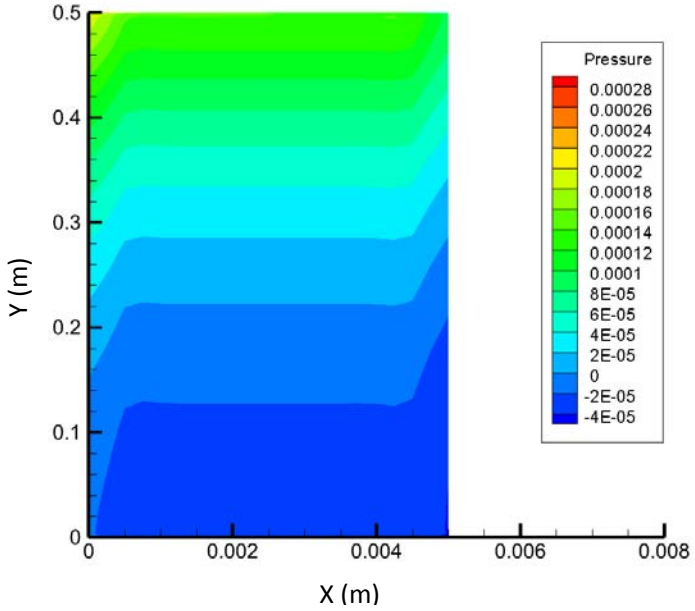

Fig. 6 Pressure distribution cloud map in air gap

It can be seen from Fig. 6 that there is a slight pressure difference at different positions in the air gap, and the pressure is close to atmospheric pressure. In the air gap, the water evaporates into water vapor and expands in volume, so the pressure near the evaporator is bigger. After the water vapor condenses, the volume decreases and the pressure near the condenser decreases. The entire air gap is in a closed state, the water vapor at the upper position evaporates, the volume expands, so the pressure is large, with the height decreases, the evaporation rate decreases, the pressure gradually decreases, and the pressure near the bottom of the air gap is negative.

Fig 7 shows the pressure distribution at the evaporator interface, the center line, and the condenser interface position in the vertical direction. As can be seen from Figure 7, the pressure in the air gap gradually decreases with height, and the pressure at the evaporator interface is greater than the pressure at the interface of the condenser, and the pressure difference between the evaporator and condenser interface decreases as the height decreases gradually. The change of pressure difference is related to the evaporation and condensation rate. The upper part of the air gap has a high temperature, and the water evaporates and condenses strongly. Therefore, the pressure difference is large. The temperature in the bottom part is lower and the phase change is weaker, so the pressure difference is smaller. In the place near the top and the bottom wall, the pressure will be abrupt change due to the influence of the wall. The pressure difference between the upper and bottom portions of the air gap encourage the internal convection.

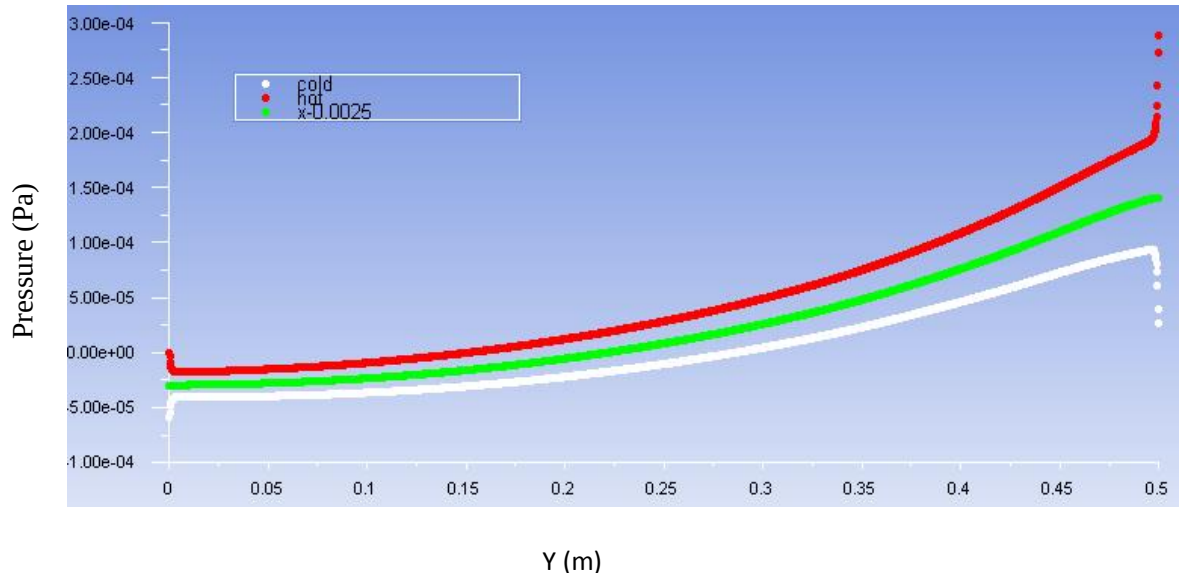

Fig. 7 Pressure distribution in height direction

As shown in Fig. 8, the distribution of the pressure at the positions of y coordinates of 0.125, 0.25, and 0.375 is shown. On the whole, in the air gap, the pressure is large on the top and small on the bottom, the pressure near the evaporator is large. At a same height, the internal pressure of the air gap away from the evaporator and the condenser does not change in the x direction, the pressure near the condenser is small. The pressure distribution characteristics are mainly influenced by the volume change of the phase transfer, the evaporator pressure is higher than the condenser pressure, and the pressure difference at the same height will push the humid air in the air gap move to the condenser. It can increase the diffusion rate of water vapor in the air gap and increase the yield of fresh water.

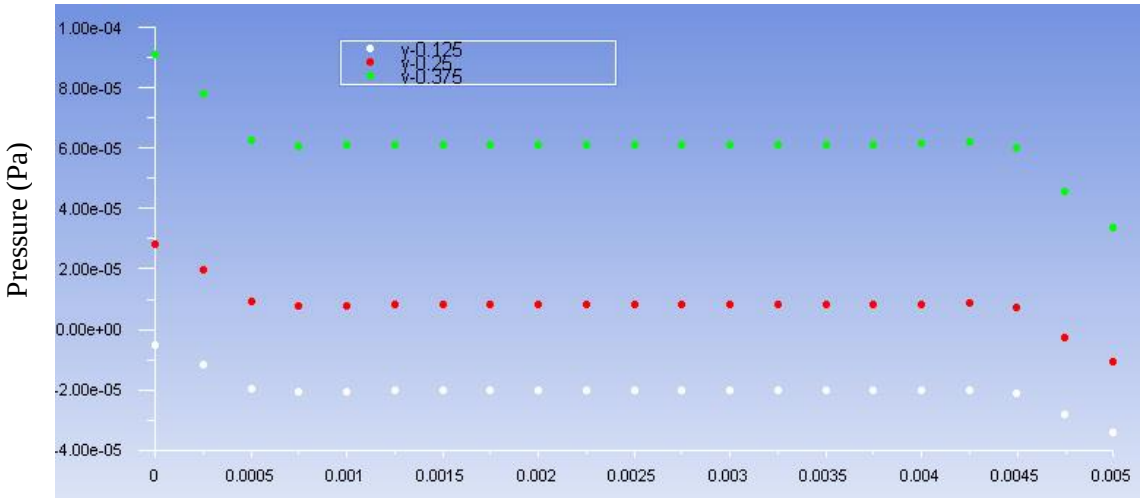

Fig. 8 Pressure distribution on different x sections

3.3 Concentration Distribution

Figure 9 shows the concentration distribution of water vapor in the air gap. It can be seen from the figure that the concentration distribution of water vapor is similar to the temperature distribution, and the water vapor

concentration at the position where the temperature is high is large. The place where the water vapor concentration is the largest is that the evaporator is close to the top, and as the height is lowered, the water vapor concentration is decreased. As the x coordinate increases, the water vapor concentration decreases.

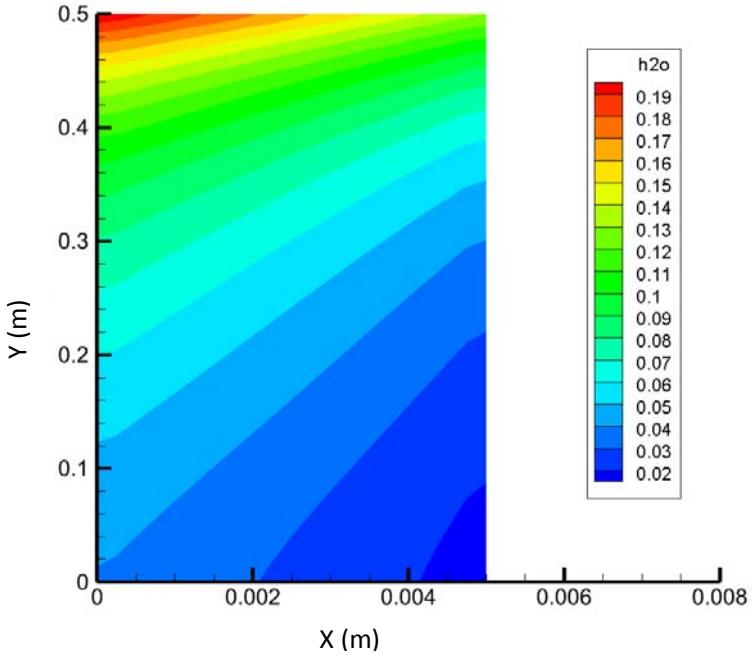

Fig. 9 Water vapor concentration distribution cloud map in air gap

Fig. 10 shows the water vapor concentration distribution on the evaporator, center line and the condenser.

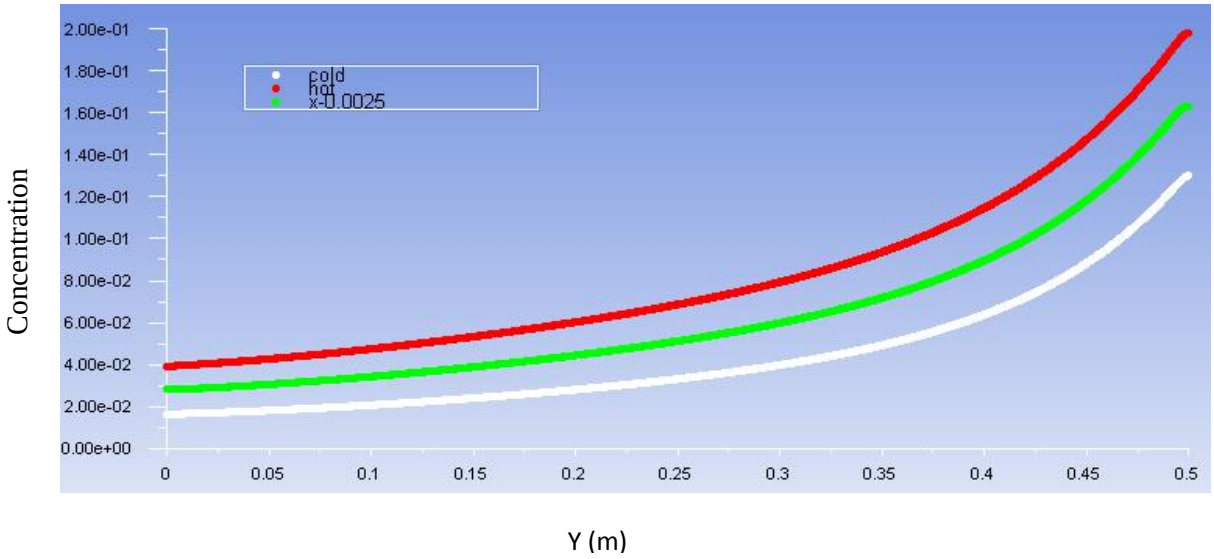

Fig. 10 Water vapor mass concentration distribution in height direction

It can be seen from the figure that as the height decreases, the water vapor concentration decreases, and the slope of the upper position concentration line is huge, the concentration changes quickly, the bottom position curve is gentle, and the concentration change is slowly. In the upper position, the concentration difference of the evaporator and the condenser is significantly greater than the concentration difference at the bottom position, because the saturated partial pressure of water vapor is an exponential function of temperature.

Under the same temperature difference, the concentration caused at high temperature is greater than the low temperature.

Fig 11 shows the water vapor concentration distribution on the three surface at y coordinates of 0.125, 0.25 and 0.375. As can be seen from Fig. 11, on the three surface, the water vapor concentration decreases as the x coordinate increases. On the 0.375 section, Concentration accumulation can be seen near the evaporator and condenser locations, and within the air gap, water vapor concentration distribution is linear. The slope of the water vapor concentration curve near the upper section is the largest, the difference of the water vapor concentration between the evaporator and the condenser surface is the largest, the slope of the water vapor concentration line on the bottom section is the smallest, and the difference of the water vapor concentration between the evaporator and the condenser surface is the smallest.

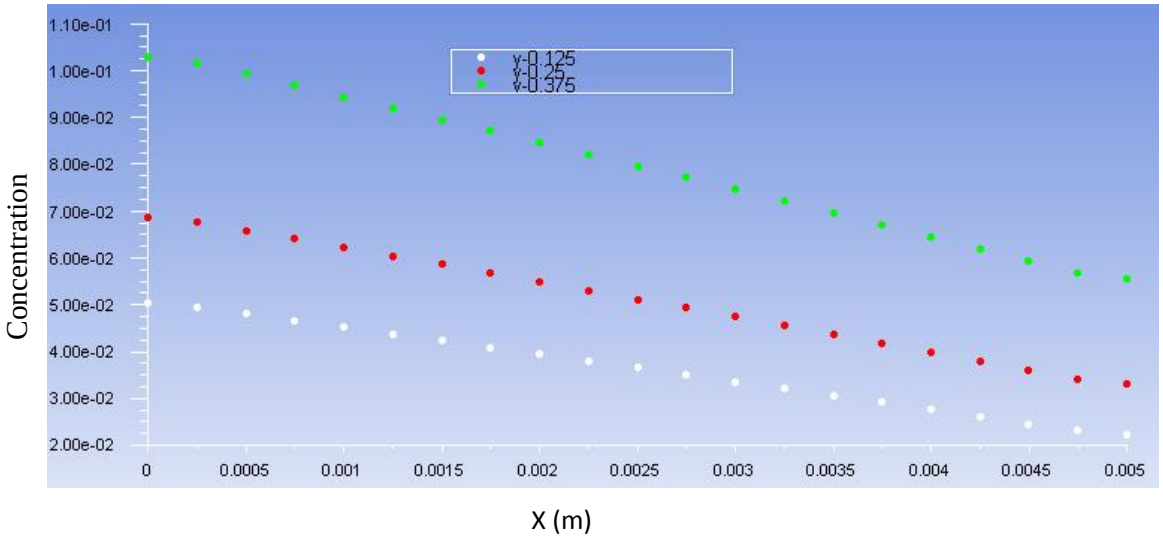

Fig. 11 Water vapor mass concentration distribution on different x sections

4. CONCLUSIONS

The temperature distribution law in air gap is top high and bottom low, left high and right low. At different heights, the temperature difference between the evaporator and the condenser same in basically, the upper part of the model evaporates strongly and the temperature drop is large. The phase change heat on the boundary between the evaporator and the condenser causes temperature difference polarization, and the polarization factor is related to the strength of the phase change.

The water at the evaporator interface evaporates and expands in volume, the pressure is large; the water vapor at the condenser interface condenses, the pressure is small; there is a pressure difference at different positions inside the air gap, and the pressure at the upper is the largest, and the pressure decreases as the height decreases; In the upper end of the air gap, The pressure difference between the evaporator and the condenser surface is the largest, and the pressure difference decreases as the height decreases.

The concentration distribution law is similar to the temperature, and the water vapor concentration decreases with the decrease of the height. The concentration near the evaporator side is large, and the concentration on the condenser side is small.

The humid air inside the air gap flow from the evaporator to the condenser, and the upper end temperature is high, and if the concentration is larger, the flow rate is quicker.

ACKNOWLEDGMENT

We are deeply indebted to the National Natural Science Foundation of China (No. 51876023, No. 51776029) for its funding, and the Liaoning Province's Natural Foundation Guidance Project (No. 20180550732).

NOMENCLATURE

A	area in the grid to phase transfer, m^2	x	horizontal direction of air-gap, m
D	diffusion coefficient of water vapor in air-gas, m^2/s	Y,y	height direction of air-gap, m
E	specific total energy, J/kg	**Greek letters**	
g	acceleration of gravity, kg/(m•s^2)	γ	latent heat of water evaporation, J/kg
h	specific enthalpy, J/kg	θ	temperature difference polarization factor, (-)
j	mass flux obtained by Fick's first law, kg/(m^2•s)	ρ	density, kg/m^3
m	total mass flux, kg/(m^2•s)	τ	stress, Pa
p	partial pressure, Pa	ω	mass fraction of the water vapor, (-)
R	rate of mass increase by chemical reaction, (-)	μ	dynamic viscosity of water vapor, Pa s
r	latent heat of water in evaporator, J/kg	**Superscripts**	
S	Source, (-)	c	condenser
Sc	Schmidt number, (-)	e	evaporator
S_h	energy source, (-)	eff	effective
S_i	component source, (-)	i	species i
S_m	mass source, (-)	j	species j
S_v	momentum source, (-)	m	mass
T	temperature, K	ref	reference
t	temperature, ℃	s	saturated vapor
V	volume, m^3	T,t	thermal
v	velocity, m/s	W	water

REFERENCES

[1] Leu J S, Jang J Y, Yin C. Heat and mass transfer for liquid film evaporation along a vertical plate covered with a thin porous layer, International Journal of Heat & Mass Transfer, 2006, 49(11):1937-1945.

[2] Ming-Hsyan S, Huang M J, Chen C K. A study of the liquid evaporation with Darcian resistance effect on mixed convection in porous media, International Communications in Heat & Mass Transfer, 2005, 32(5):685-694.

[3] Yiotis A G, Boudouvis A G, Stubos A K, et al. Effect of liquid films on the drying of porous media, Aiche Journal, 2004, 50(50):2721-2737.

[4] Shirazian S, Ashrafizadeh S N. 3D Modeling and Simulation of Mass Transfer in Vapor Transport through Porous Membranes, Chemical Engineering & Technology, 2013, 36(1):177-185.

[5] Tang N, Zhang H, Wang W. Computational fluid dynamics numerical simulation of vacuum membrane distillation for aqueous NaCl solution, Desalination, 2011, 274(1):120-129.

[6] Wang L, Wang H, Li B, et al. Novel design of liquid distributors for VMD performance improvement based on cross-flow membrane modul, Desalination, 2014, 336(3):80-86.

[7] Ma Le. Research on solar desalination plant, Xian, Chang 'an University, 2010.

[8] Liu Jun. Simulation of the microscopic characteristics of pressure reducing membrane distillation process, Tianjin, Tianjin University, 2015.

[9] Liu Jun,Li Anbao. Simulation analysis of thermal mass transfer characteristics of fiber membrane surface in pressure reducing membrane distillation process,Chemical Industry and Engineering, 2016, 33(6):80-87.

[10] Xu Kai, Li Anbao. CFD numerical simulation of flow field in a new plate-frame air gap membrane distillation module, Membrane Science and Technology, 2017, 37(2):88-95.

[11] Fang Da. Numerical analysis on condensation and convection heat transfer characteristics of gas-vapor mixture, Jinan, Shandong University, 2014.